ARCHER

Collaborative Project

Co-funded by the European Commission under the
Euratom Research and Training Programme on Nuclear Energy
within the Seventh Framework Programme

Grant Agreement Number: 269892
Start date: 01/02/2011 Duration: 48 Months

www.archer-project.eu

Modelling of dust behavior in HTR confinements during depressurization accidents with COCOSYS

Stephan Jühe (RWTH)

ARCHER project – Contract Number: 269892
Advanced High-Temperature Reactors for Cogeneration of Heat and Electricity R&D
EC Scientific Officer: Dr. Panagiotis Manolatos

Document title	Modelling of dust behavior in HTR confinements during depressurization accidents with COCOSYS
Author(s)	Stephan Jühe (RWTH)
Number of pages	25
Document type	Deliverable
Work Package	WP23
Document number	D23.61 – revision 0
Issued by	RWTH
Date of completion	26/06/2012
Dissemination level	Restricted to the partners of the ARCHER project

Summary

This document contains a description and results of the efforts to simulate dust behavior in the confinement of the HTR-Module 200 during a depressurization accident.

Approval

Rev.	Short description	First author	WP Leader	SP leader	Coordinator
0	First revision	S. Jühe 26/06/2012	K Verfondern (IKE) 31/10/12	N. Kohtz (TUV) 31/10/12	S. de Groot (NRG) 31/10/12

Distribution list

Name	Organisation	Comments
P. Manolatos	EC DG RTD	
All technical participants	ARCHER	
Steering Committee members	ARCHER	

Table of contents

1 Nomenclature

Abbreviation	Meaning
AFP	Aerosol Fission Product Behavior (module for COCOSYS)
ASTEC	Accident Source Term Evaluation Code
AVR	Arbeitsgemeinschaft Versuchsreaktor
CCI	Core Concrete Interaction (module for COCOSYS)
COCOSYS	Containment Code System
DIREKT	Thermal-Fluid code with direct solver
FFE	Pipe for fuel feed equipment
FIPLOC	Containment simulation program
GRS	Gesellschaft für Anlagen- und Reaktorsicherheit
HTR	High Temperature Reactor
KLAK	Kleine Absorber Kugeln (small absorber spheres)
KOAX	Coaxial duct
PEL	Pressure equalization line
RALOC	Radiolysis and local gas gas concentration
SPECTRA	Sophisticated Plant Evaluation Code for Thermalhydraulic Response Assessment
STAR	Staubtransport, -ablagerung und resuspension (dust transport, deposition and resuspension)
THTR	Thorium Hochtemperaturreaktor
THY	Thermal Hydraulics (module for COCOSYS)

Symbol	Unit	Meaning
d	m	Particle diameter
q_0	$\frac{1}{m}$	Distribution density: number weighted
q_3	$\frac{1}{m}$	Distribution density: mass weighted
R_{red}	-	adhesive reduction due to surface roughness
$\dot{q}''$	$\frac{W}{m^2}$	Heat flux
Sc	-	Schmidt-number
∇T	$\frac{K}{m}$	Temperature gradient
T_W	K	Wall temperature

T_{fl}	K	Fluid temperature
u_τ	$\frac{m}{s}$	Friction velocity
$v_{dep,turb}$	$\frac{m}{s}$	Deposition velocity for turbulent deposition
α	$\frac{W}{m^2\,K}$	Heat transfer coefficient
ρ_{fl}	$\frac{kg}{m^3}$	Fluid density
λ_{fl}	$\frac{W}{m\,K}$	Thermal conductivity of the fluid
η	$\frac{kg}{m\,s}$	Dynamic viscosity
σ_g	-	geometric standard deviation of the adhesive forces
τ	s	Relaxation time
τ^+	-	Dimensionless relaxation time

2 Introduction

Carbonaceous dust is formed during normal operation of HTR due to several mechanisms. Because it interacts with fission- and activation products, this dust is a significant activity carrier. It is deposited on primary circuit surfaces, from which it can be resuspended during depressurization accidents. Current HTR-concepts will not be provided with a gas tight containment, but with a “filtered/vented confinement” from which gases will be released into the atmosphere in case of a significant break in the primary circuit. Thus, certain amounts of dust will exit through the breach of the primary circuit and eventually from the confinement into the environment. The analysis of that source term chain for dust has been considered as a major safety issue for HTR [INL11a] , [JÜH12]. Within this deliverable, the status of the work undertaken to simulate dust behavior in the confinement of a selected HTR reference plant is presented.

3 Choice of reference plant

Because dust behavior depends on plant geometry and fluid dynamic conditions, its analysis cannot be performed for HTR in general, but only with respect to a specific reference plant.
Due to its technical maturity, its still existing relevance for current HTR projects and the availability of detailed information on plant design, the HTR-Module-200 in its 2-Block layout was selected as the reference plant for the analysis presented here.
A comprehensive plant description is given in [INL11b].

3.1 Plant description

3.1.1 Primary circuit

A large fraction of the primary circuit volume of $460\ m^3$ takes part in the normal operation helium circulation. A simplified illustration of the gas flows is given in figure 1.

Passing through the pebble bed (1), the helium is heated to a medium temperature of 700 °C. It then flows through bores in the bottom reflector (2) and mixing chambers into the torus-shaped hot gas collector (3). From there, it is led through the inner tube of the coaxial duct (4) into the steam generator (5). Heat is transferred to the steam generator tubes, cooling the gas to 250 °C. From there, it flows to the blower (6), which generates the differential pressure of $0{,}15\ MPa$ necessary to maintain helium circulation against the flow resistance. Through the outer part of the coaxial duct the gas gets to the annulus (7) between reactor pressure vessel and core barrel. After passing the bottom of the reactor pressure vessel, the helium then flows through the side reflector (8), a small cavity above the top reflector (9) and through bores into the space above the pebble bed.

Additionally, the primary circuit also features volumes with stagnating helium. These are especially the gas plenum in the upper calotte of the reactor pressure vessel (a) and the cavity between top reflector and thermal shield (b), but also the annuli between reactor pressure vessel and core barrel (c) as well as core barrel and side reflector (d) and the structures (e) containing the discharge vessels of the KLAK system.

Through the outer pressure compensation line, the outer annulus is connected with the blower-buffer. Additionally, the gas plenum in the upper calotte of the reactor pressure vessel is connected with the cold gas-filled region via the inner pressure compensation line, which is closed during normal operation by a rupture disc and allows for the gas to exit during a depressurization accident with the intention of preventing destructive pressure differences over the core structures.

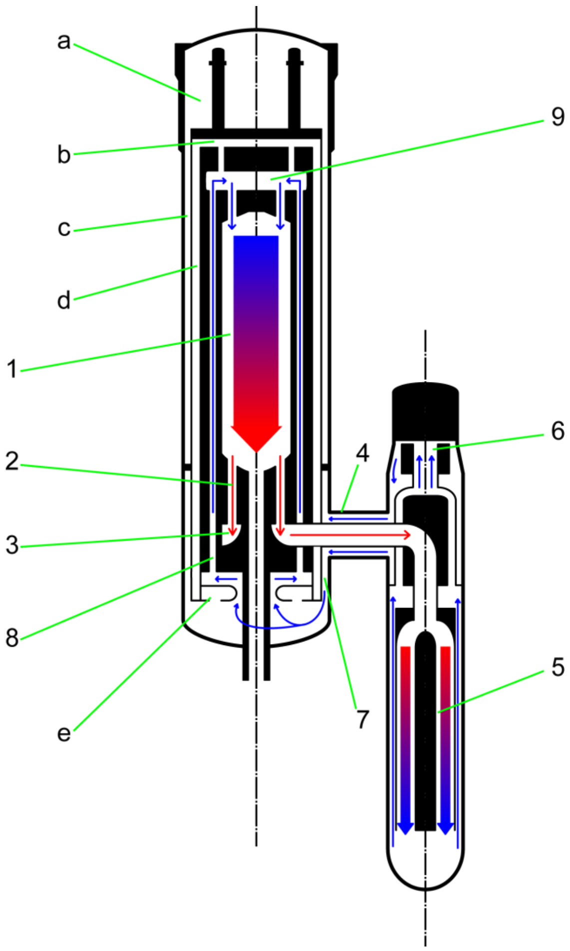

Figure 1: Helium flow in the HTR-Module

3.1.2 Confinement

A schematic of the plant geometry with respect to the pressure relief path is shown in figure 2. The reactor and steam generator cavity surrounding the primary circuit are connected with a relief opening to the fuel handling room, which in turn communicates with the rooms of the module block on the $-9{,}55\ m$ level. Up to the $+9{,}50\ m$ level, the gas can flow freely within the rooms of the module block. The upper part is connected to a pressure relief duct, which is closed by a rupture disk during normal operation and leads into the reactor building at approx. $+28\ m$. Because of relief openings at $+31{,}9\ m$, leading to the flue, a significant part of the volume of the reactor building is not part of the depressurization flow path. On the $\pm 0\ \mathrm{m}$ level, a door opening at overpressure connects the reactor building to the rooms of the other module block as well as two stairwells.

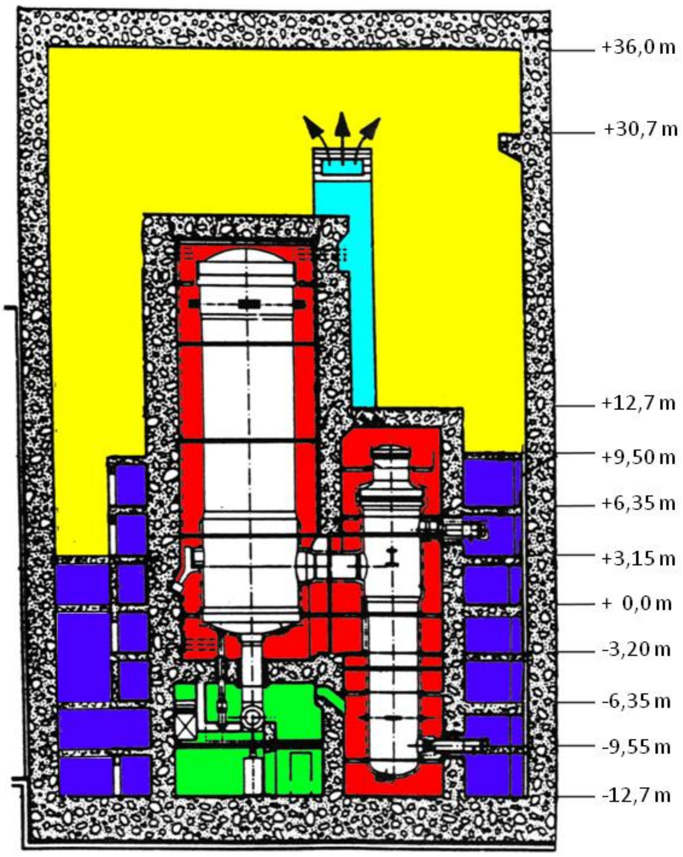

Figure 2: Schematic illustration of the volumes relevant for depressurization for the HTR-Module (modified from [INT679])

3.2 Description of break in the primary circuit

The location of the leaks assumed in [JÜH11] for the HTR-Module are shown in Figure 3. The components designated by the abbreviations are the pressure equalization line (PEL), pipe for fuel feed equipment (FFE) and the coaxial duct (KOAX).

A break of the PEL has been considered a design basis accident for the HTR-Module. On the other hand, breaks of FFE and KOAX have been excluded as DBA; however, as beyond design basis accidents, their analysis is still of interest for nuclear safety research.
For the sake of brevity, only the case of the break of the PEL is presented in this deliverable; the differences between PEL and FFE are only quantitative, while for KOAX, no meaningful analysis of dust behavior is possible because of the severe destruction caused by such a break. [JÜH11]

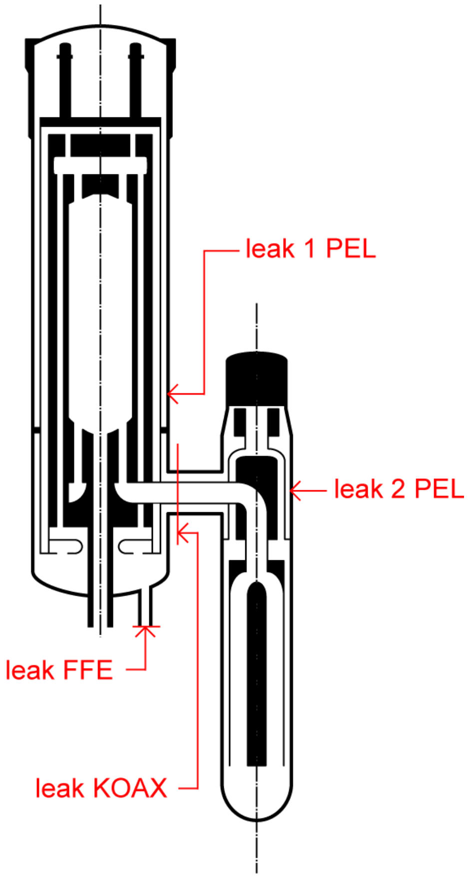

Figure 3: Locations of possible leaks

4 Choice of reference dust

In order to be able to make quantitative predictions about the dust bound source term for the HTR-Module, existing knowledge about dust in pebble bed HTR has been refined.

4.1 Dust amount

When transferring experience with dust produced in the AVR and THTR reactors (which however is afflicted with uncertainties) to other plants, e.g. thermal power or the number of fuel element cycles can be used as a scaling factor. Additionally, an experimentally determined production rate of 10 mg dust per fuel handling is stated for the HTR-Module [IAE97]. Altogether, there is no evidence contradicting the original prediction of an overall dust production of 500 – 1000 kg for the HTR-Module within 32 full power years [INT87/88], [SCE88]. For the scope of the analysis presented in this deliverable, the upper limit of 1000 kg has been premised consistent with other work. [JÜH11], [JÜH12]

4.2 Dust particle size and morphology

For all aspects of dust behavior, its size distribution is of great importance. The dimensions of non-spherical particles can be determined and described by various methods, yielding results that cannot be directly compared.

Unfortunately, most of the sources cited here do not take that into account – the characterization of dust is performed just by the particle diameter without further information. Only in [FAC08b], it is given as the diameter of a circle of identical projection area as the particle; a systematic analysis of particle morphology is not documented, either.

Due to the lack of substantiated information for the morphology of HTR-typical dust particles, for the scope of the work presented here they are assumed to be massive and spherical. This simplification was also used by [FON09].

A theoretical prognosis of the particle sizes produced by abrasion is not possible at the present state of knowledge. Since no definite answer can be given to the question of the dominant production mechanism for carbonaceous dust anyway, and the results of abrasion experiments for dust production are not assured to reflect actual HTR conditions (see section 1.2.1), the determination of the particle size spectrum solely depends on HTR operation experience.

Three sources were utilized for the determination of particle size distribution:

1. AVR dust analyzed 20 years after shutdown [FAC08a]
2. AVR dust analyzed during reactor operation [GOT90]
3. THTR dust [OET89]

The corresponding size distributions are shown in figures 4-6. Due to counting statistics, the data for mass weighted distributions for the AVR dust is problematic because of the very low frequency of big particles in the original number weighted distribution given in the sources.

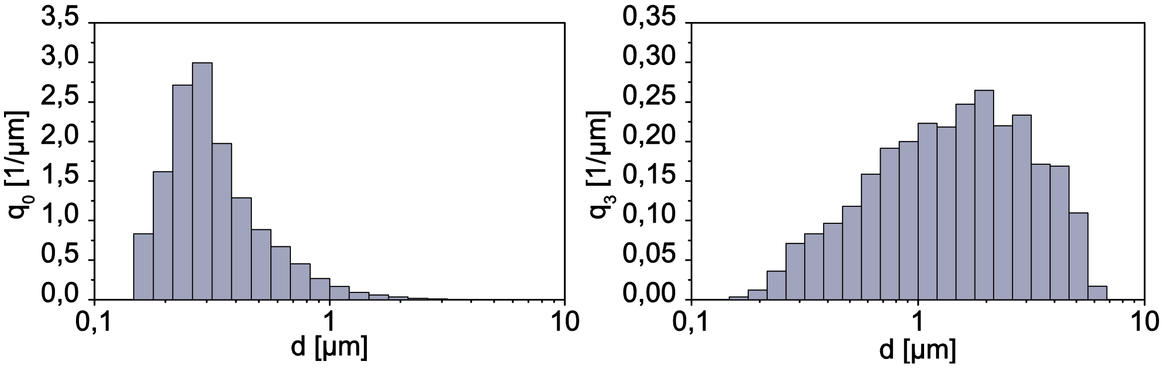

Figure 4 : Particle size distribution density for AVR dust according to [FAC08a] / [FAC08b] :
Number weighted (left) and mass weighted (right)

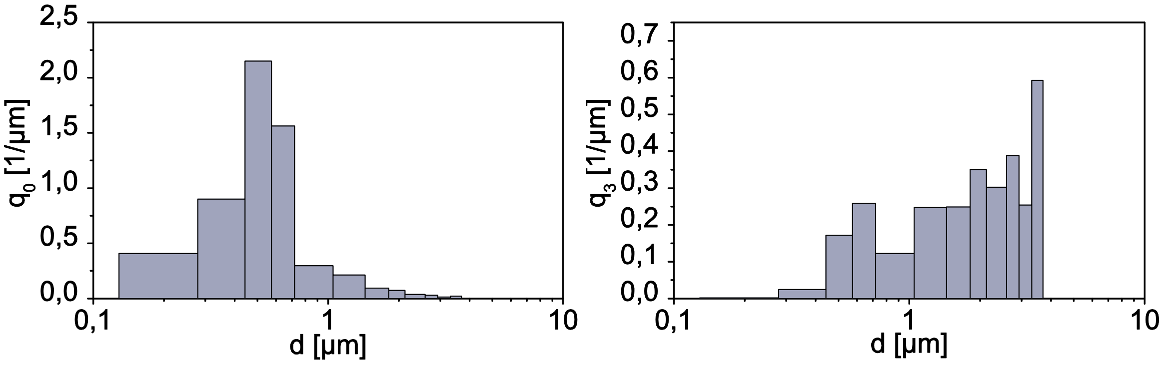

Figure 5 : Particle size distribution density for AVR dust according to [GOT90] :
Number weighted (left) and mass weighted (right)

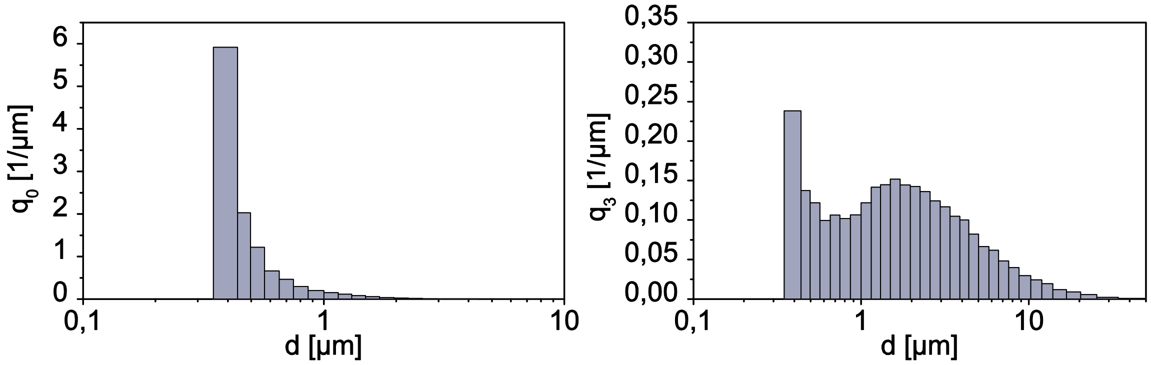

Figure 6 : Particle size distribution density for THTR dust according to [OET89] :
Number weighted (left) and mass weighted (right)

Since it is not possible to make a universal statement whether an under- or overestimation of particle size can be considered conservative for depressurization events, the data from the three sources presented above is used to define the particle size distribution scenarios S1 to S3.
For the use in COCOSYS, the number of particle size classes is limited to 20; except for absolute upper and lower limit, the discretization is determined internally.

The characterization of HTR dust for all 3 scenarios is given in table 1 and figure 7.

Table 1: Dust particle size distributions

Size class				fraction S1 [mass %]	fraction S2 [mass %]	fraction S3 [mass %]
#	d^{min} [µm]	d^{max} [µm]	d^{lm} [µm]			
1	0.1000	0.1413	0.1189	0.0000	0.0022	0.0000
2	0.1413	0.1995	0.1679	0.0372	0.0101	0.0000
3	0.1995	0.2818	0.2371	0.3318	0.0217	0.0000
4	0.2818	0.3981	0.3350	0.9453	0.2830	1.2012
5	0.3981	0.5623	0.4732	1.7963	2.1713	2.5595
6	0.5623	0.7943	0.6683	4.0525	4.8836	2.3936
7	0.7943	1.1220	0.9441	6.8056	4.9169	3.6449
8	1.1220	1.5849	1.3335	10.4858	11.4719	6.6520
9	1.5849	2.2387	1.8836	16.5958	20.0589	9.4792
10	2.2387	3.1623	2.6607	21.0460	29.6483	11.7314
11	3.1623	4.4668	3.7584	22.1873	26.5321	13.5132
12	4.4668	6.3096	5.3088	14.8646	0.0000	12.8436
13	6.3096	8.9125	7.4989	0.8517	0.0000	11.6634
14	8.9125	12.5893	10.5925	0.0000	0.0000	9.3483
15	12.5893	17.7828	14.9624	0.0000	0.0000	6.8651
16	17.7828	25.1189	21.1349	0.0000	0.0000	4.9354
17	25.1189	35.4813	29.8538	0.0000	0.0000	2.0808
18	35.4813	50.1187	42.1697	0.0000	0.0000	1.0885
19	50.1187	70.7946	59.5662	0.0000	0.0000	0.0000
20	70.7946	100.0000	84.1395	0.0000	0.0000	0.0000

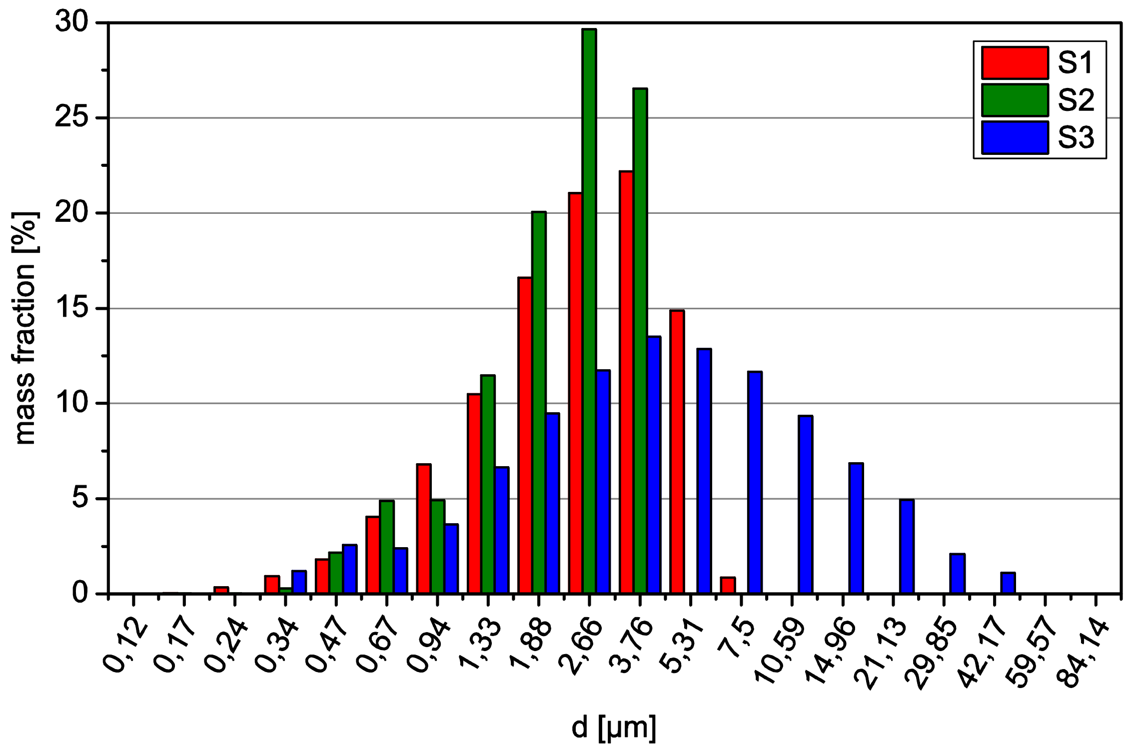

Figure 7: Dust particle size distributions

5 The COCOSYS code

Based on several codes, among others RALOC and FIPLOC, the German GRS develops the containment code system COCOSYS [ALL08]. The goal is to be able to simulate all containment phenomena following design basis accidents as well as severe accidents of light water reactors through mechanistic models [KLE10].

5.1 General description / Thermohydraulics

The principal modules of COCOSYS are THY (Thermal Hydraulic) and AFP (Aerosol and Fission Products); an additional module CCI (Corium Concrete Interaction) is not needed for most applications.
As a "lumped parameter code", COCOSYS requires the geometry to be divided into several (depending on the application 20-200), zero-dimensional zones, which thermohydraulically interact via junctions. The zones can be subdivided into several zone parts, which, however is relevant mainly for scenarios involving liquid water as well as gas flows and therefore negligible for depressurization accidents of HTR.
Flow resistance occurs at the junctions connecting the individual zones, thus together with the driving forces (pressure differences) determining the gas flow between the volumes. Additionally, models for components like rupture disks or flaps are included into the junction calculation.
Heat transfer to walls and through walls between different zones can be simulated through the modeling of heat conducting materials in a feature called "structures".
The thermohydraulic influence of different accident management measures can be simulated in COCOSYS, too; due to their irrelevance for HTR depressurizations, their description is omitted here.

5.2 Aerosol/Dust Models

For the simulation of aerosol and fission product behavior, several mechanisms are taken into account, of which only the ones relevant for the task at hand are described here:
Aerosol-related calculations are performed for each zone. The particle size range is discretized into several (up to 20) particle size classes. Particles can be deposited on walls; the mechanisms modeled in COCOSYS are:

- Sedimentation
- Diffusive deposition
- Thermophoresis
- Diffusiophoresis

Additionally, agglomeration of particles is considered. Resuspension from dry surfaces can be calculated according to the Fromentin model; its implementation is, however, only applicable to events like hydrogen deflagrations or steam explosions.

6 Modelling the depressurization accident

Due to the scope of this deliverable, the focus of the presentation of the work performed is on the modeling of the depressurization accident in COCOSYS. The COCOSYS calculations require injection tables both for the gas and the dust entering the confinement through the breach of the primary circuit. Thus, a complete simulation of fluid dynamics and dust behavior in the primary circuit is a prerequisite to any subsequent work. A short overview of the work preceding the COCOSYS-modeling, taken from [JÜH12], is give here for better understanding.

While for the simulation of the fluid dynamics, an enhanced version of the DIREKT code developed at FZ Jülich was used, for dust behavior, a comprehensive code STAR (Source Term due to Aerosol Resuspension) was developed and coupled with DIREKT.

“The STAR code incorporates correlations for deposition, surface interaction, resuspension and transport of dust.

Mechanisms identified as relevant for dust deposition in the not stagnating volumes of the primary circuit are thermophoresis, diffusion, impaction and turbulent deposition. Thermophoresis is calculated according to the Talbot-equation [TAL80], [AHM98] and turbulent deposition with the correlation according to [WOO81]. Diffusive deposition and impaction at bends/deflection plates is calculated with the respective correlations given by [HIN99]. For impaction in the pebble bed and on the steam generator pipe bundle, the correlations from [GOR82] and [HER07] are used respectively. For turbulent flow, turbulent deposition is calculated for these geometries according to [WOO81], too, while for laminar flow, the correlations used are taken from filter efficiency calculations [ING81], [LÖF88].

The average adhesive force of dust particles on the surface was calculated with the Derjaguin-Muller-Toporov-(DMT) Model [CAR05]. The degree of variation of the adhesive forces was characterized with the geometric standard deviation σ_g. The adhesive reduction due to surface roughness (for definition: [REE01]) was incorporated through a particle-size-independent reduction factor R_{red}. Since dust deposits in AVR were observed as hard and crust-like [FAC08a], surface-bound dust was modeled as the original primary particles without any formation of resuspendable clusters. Multi-layer effects were taken into account to the extent that only the uppermost part of the deposit, expressed through the free-fraction θ, is allowed to interact with the fluid.

For the simulation of dust resuspension, the quasi-static Rock’n Roll model [REE01] was selected because of its sound theoretical foundation and simplicity of application. Its implementation is similar to the SPECTRA code [STE10a]; however, no parts of the resuspension rate equation were left out for simplification reasons. The compliance with the model’s limit of validity (notably, turbulent flow conditions and the validity limits of the aerodynamic force correlations) is monitored by the code.
Dust transport was calculated considering the interaction of deposition, resuspension and convective transport, the latter being imposed by the mass flows calculated by the thermal hydraulics code DIREKT.

A more detailed description of the work performed for the development and validation of STAR and the modeling of the primary circuit of the HTR-Module for the calculation of normal operation and depressurization events is given in [JÜH11]." [JÜH12]

It should be noted that the reason "simplicity of application" for selecting the quasi-static Rock'n Roll model is not simply a matter of convenience, but rather a reference to its advantages of being dependent on very few parameters to be determined and of requiring only a modest numerical effort. The top-layer thickness for the calculation of θ was found to have little effect on integral resuspension; typically, a value of $1\,\mu m$, representing the smaller particles of the dust spectrum, was used.

6.1 Confinement model

The COCOSYS-Model for the rooms of the confinement of the HTR-Module was generated based on manufacturer information. It is illustrated in figure 8 in a compacted view, for which the zones of the reactor building and the stairwells were merged.

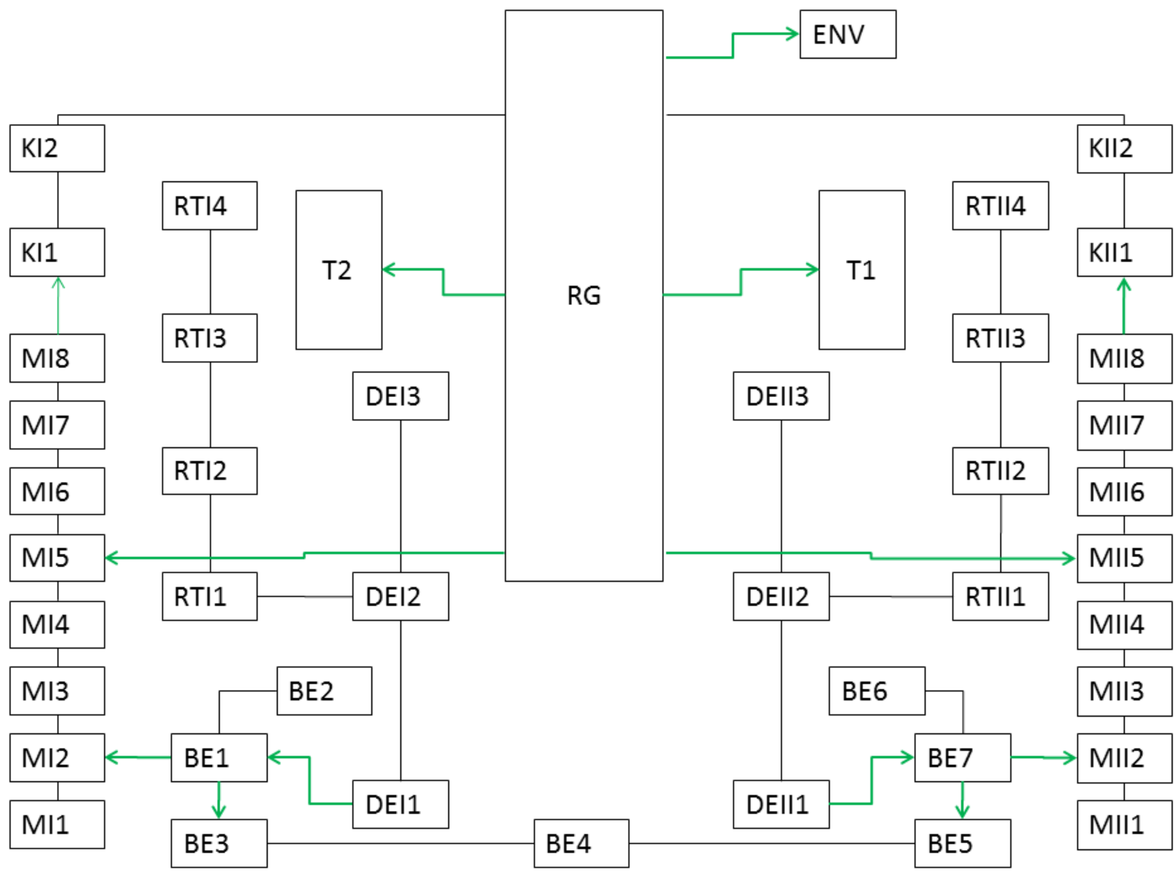

Figure 8 : COCOSYS nodalization of the rooms of the HTR-Module
(compacted view, see Table 2 for explanation)

An overview of the general configuration of the zones comprising the reactor building is shown in figure 9. Here, yellow stands for the reactor floor, green for the steam generator floor, red for the erection shaft and blue for the main transport route. For the sake of clarity, the connection of the zones through atmospheric junctions is illustrated merely by positioning them adjacently.

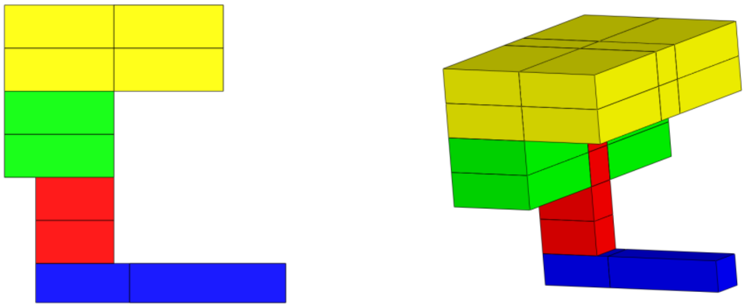

Figure 9 : Illustration of the COCOSYS nodalization of the reactor building

A breakdown of the abbreviations used is given in table 2. In the nodalization scheme, atmospheric junctions are indicated with a simple black line, while a green arrow (indicating the opening direction) stands for a rupture disk- or flap junction.

Table 2: Explanation of the zone designations for the COCOSYS nodalization

First digit		Second digit		Third digit
Abbrev.	Meaning	I	Block 1	Running number
RT	Reactor cell	II	Block 2	
DE	Steam generator cess			
BE	Fuel element handling room			
M	Rooms of module block			
K	Pressure relief duct			
T	Stairwell			
RG	Reactor building			
ENV	Environment			

Due to the significant differential pressures occurring during depressurization, for all junctions with rupture disks or flaps the ORIFICE-Model, in all other cases the INST-Model are used.
Considering the short simulation time of 500 seconds, heat conducting structures representing the concrete surfaces were defined for each zone bordering to a wall area, but no heat transfer between the zones through these structures was introduced.

6.2 Dust injection

A crucial issue for the simulation of dust behavior in the primary circuit is the determination of the parameters characterizing the adhesive forces, σ_g and R_{red}. Since for graphite dust, the experimental results from [REE01] could be reproduced with $R_{red} = 15$, $\sigma_g = 5.0$, these values were considered the expected case. Additionally, a variation study was performed from $R_{red} = 7.5 \ldots 200$ and $\sigma_g = 2.0 \ldots 5.0$.
The results for the integral dust mass exiting the primary circuits through the leak in the pressure equalization line are shown in figure 10 a-c for dust particle size distribution scenarios S1 to S3, respectively.

The results show that there is no clear correlation between lower average adhesive forces and higher dust release; sometimes it is even contrarian. This can be explained by the fact that areas exposed to high shear velocities during depressurization also face significant gas flow during normal operation, resulting in lower dust deposition for low-adhesion scenarios.

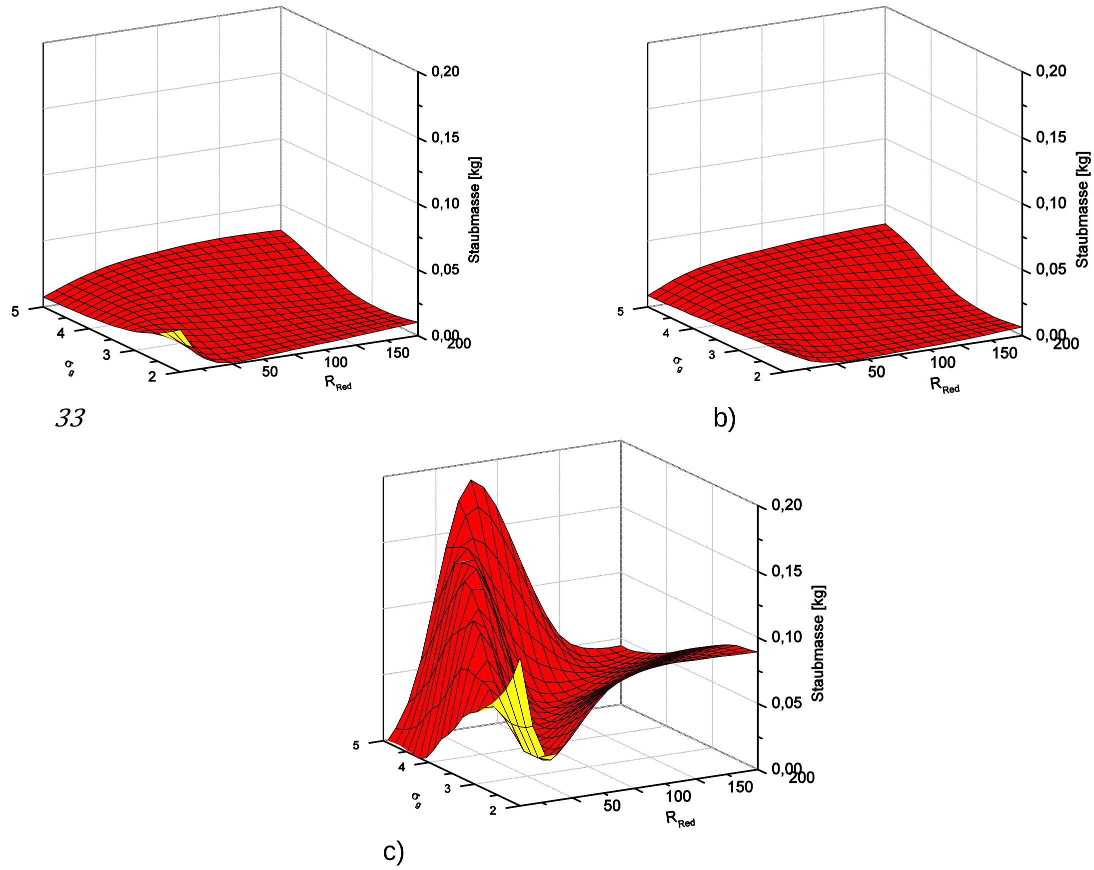

Figure 10: Dust release out of the break of the pressure equalization line as a function of adhesive force parameters for

a) Dust particle size distribution scenario S1
b) Dust particle size distribution scenario S2
c) Dust particle size distribution scenario S3

Since the focus of this deliverable is the modeling of dust behavior with COCOSYS and not an uncertainty analysis for the dust source term into the environment, only the dust injection into the confinement for the expected case is considered in the following analysis.

7 Analysis of Results

7.1 Results for calculated dust behavior

The effect of the confinement for dust retention calculated with the COCOSYS model and based on the gas and dust injection provided by the DIREKT/STAR simulation for the break of the pressure equalization I and the expected case of dust adhesive force parameters is summarized in table 3.

Table 3: Confinement dust balance for dust particle size distribution szenarios S1-S3

	S1	S2	S3
Total dust mass injected into confinement	$10.2\ g$	$11.9\ g$	$6.4\ g$
Total dust mass released into ENV	$3.5\ g$	$4.1\ g$	$2.1\ g$
Released fraction	34 %	35 %	33 %

Generally, it can be stated, that while some of the dust is retained in the confinement, a significant amount still escapes into the environment. The influence of the deposition of dust on the released fraction is illustrated in figure 11 for particle size distribution scenario S3. In that graph, the relative dust mass released into ENV stands for the ratio of the mass released up to that simulation time into the environment and the respective value at the end of the depressurization. The fraction of the deposited dust mass refers to the cumulated dust mass injected into the confinement at the corresponding time.

It can thus be stated that the retention of dust in the confinement is almost solely based on the remaining of dust laden gas inside the building after pressure equalization. For the other scenarios S1 and S2, deposition is slightly lower than for S3 - the minor differences do not necessitate additional figures. Any influence of particle size distribution on release behavior is mainly due to differences in the remobilization from the primary circuit as shown in figure 10. Dust deposition in the confinement is generally low and mostly only takes place after a major part of release into the environment has already occurred.

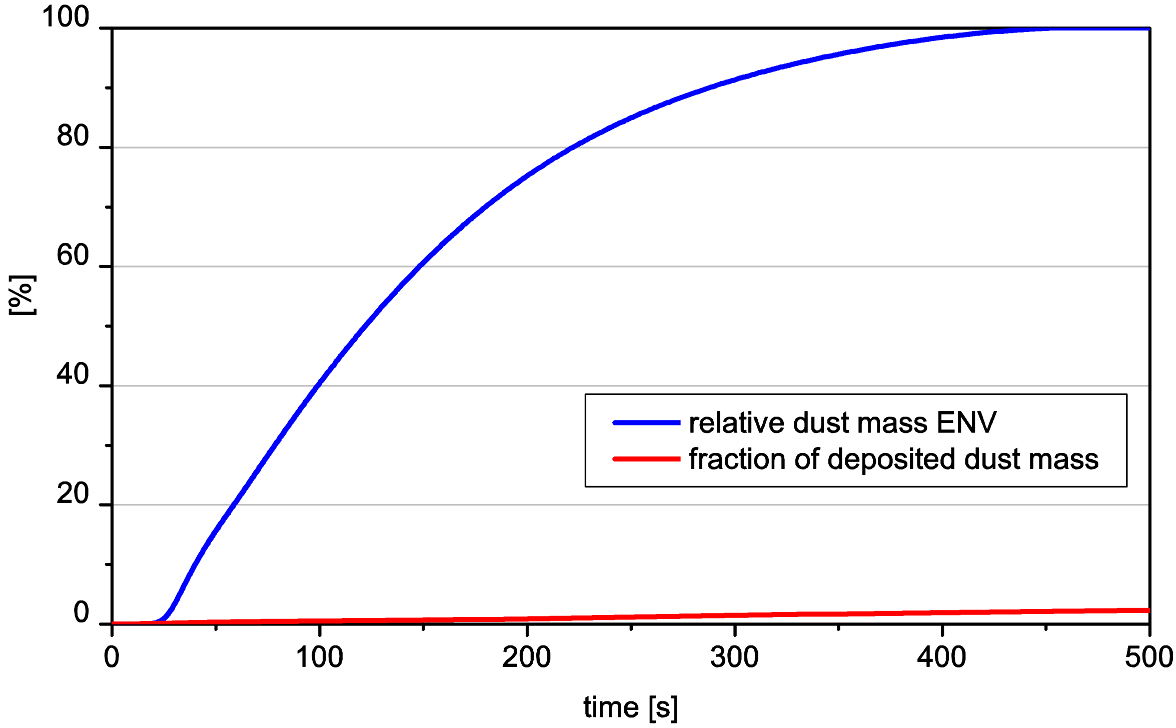

Figure 11: Relative dust release and deposition for dust particle size distribution scenario S3

The relative fraction of each dust particle size class is compared for the dust produced during reactor operation, the dust entering the confinement from the leak and the dust eventually released into the environment for the scenarios S1-S3 in figures 12-14. Since the objective is to analyze size distribution, no conclusions to the relations of the total dust masses involved must be drawn from this illustration. It has to be pointed out that both “release” values were obtained through integration over the whole depressurization; additionally, there is a significant time dependence of the spectrum of the dust leaving the primary circuit.

Generally, the influence of the confinement on the dust spectrum is marginal. The observable trend to a higher proportion of smaller particle diameters (compared to the dust originally produced in the reactor) is mainly due to the corresponding injection rates. The fact that most of the dust mass relevant as a potential environmental concern has a particle size between approx. $0.5\ \mu m$ and $5\ \mu m$ can serve for a first approach for devising solutions for dust precipitation.

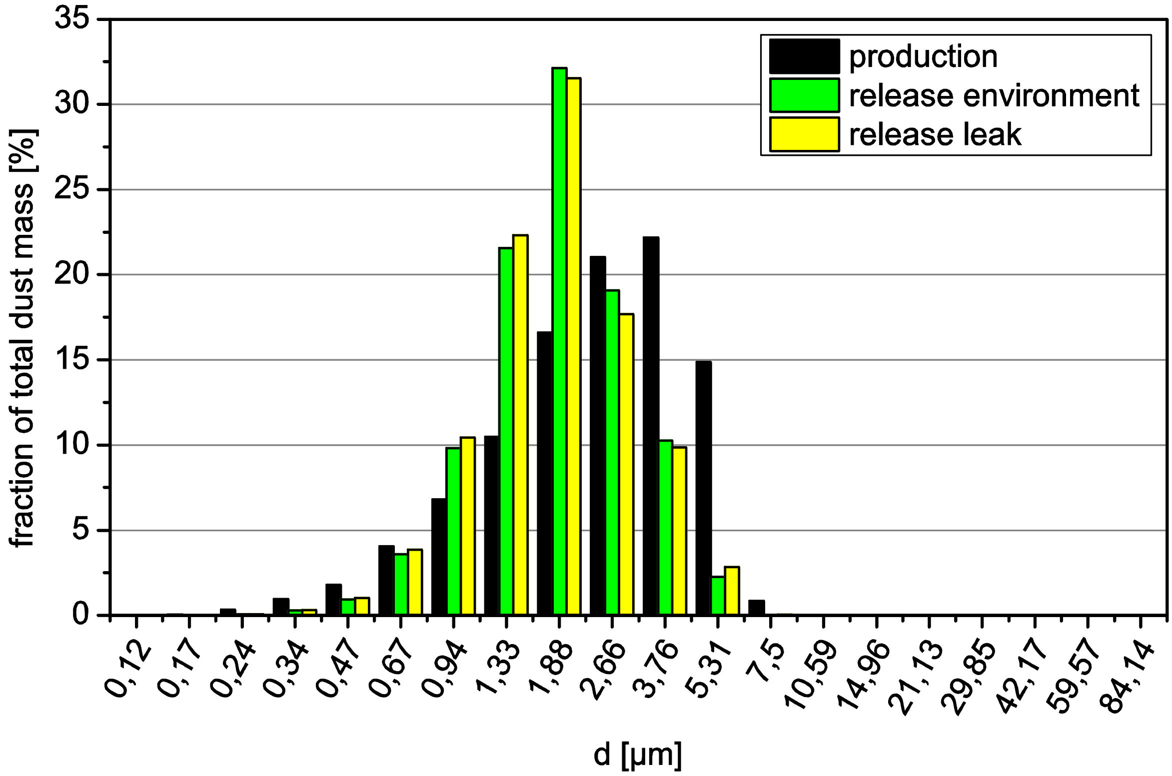

Figure 12: Dust spectrum comparison for scenario S1

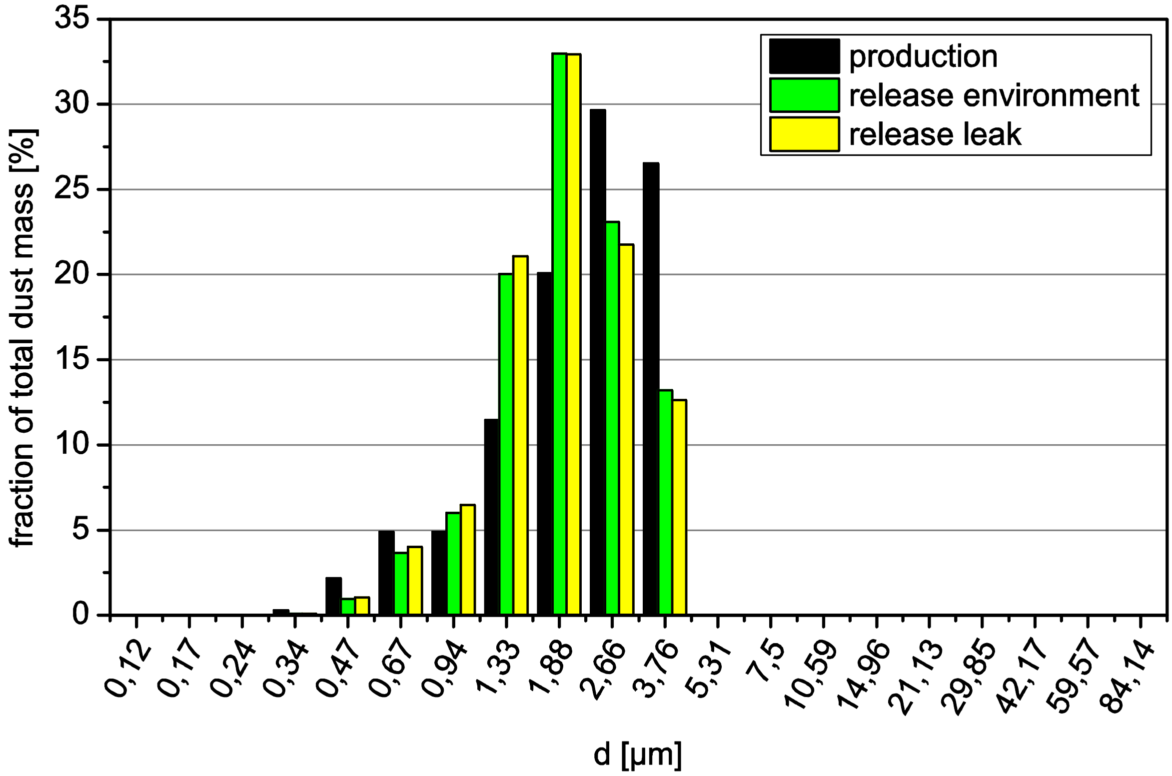

Figure 13: Dust spectrum comparison for scenario S2

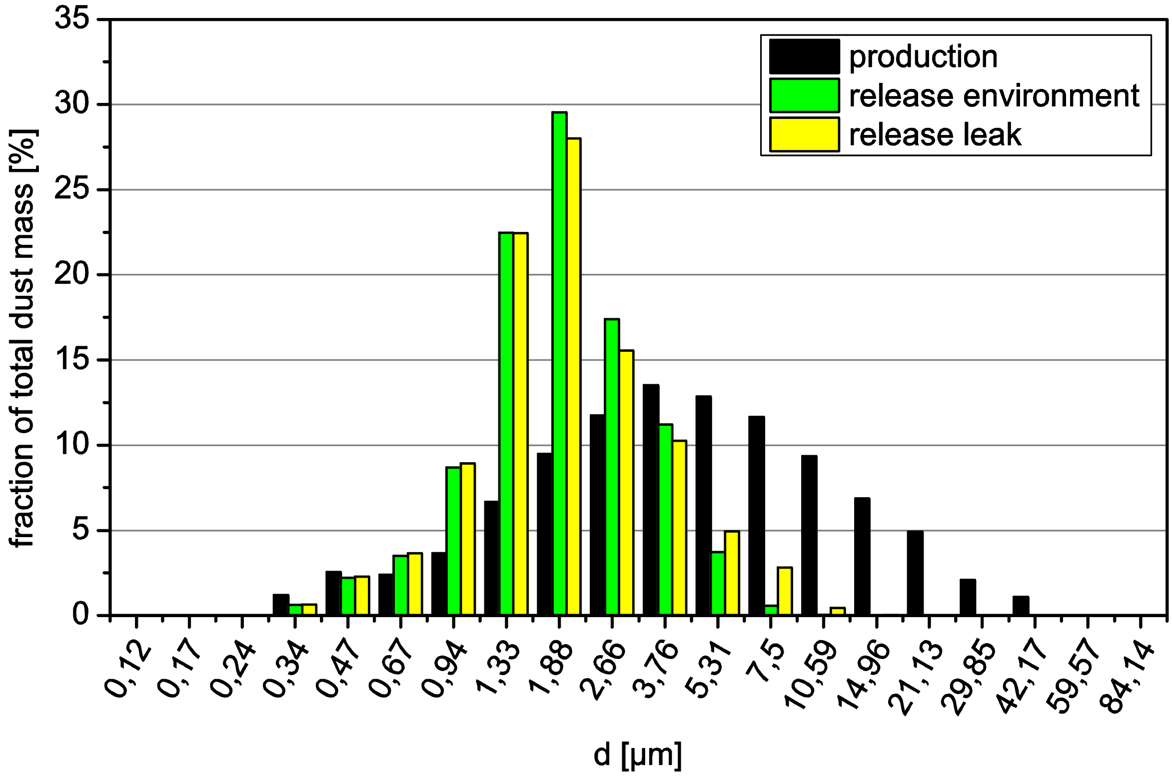

Figure 14: Dust spectrum comparison for scenario S3

7.2 Identified potentials for improvements

The results presented in chapter 4.1 were obtained with the “as is” Version 2.4 beta of COCOSYS. During the work performed, several issues were identified which should be considered for further analysis’ of dust behavior in the confinement with that code system.

7.2.1 Turbulent deposition

Turbulent deposition is a generic term for several mechanisms carrying particles through the vicious sublayer of a turbulent flow, most notably diffusion and eddy impaction [HIN99].

Currently, no model for turbulent deposition is implemented in COCOSYS. A simple correlation for deposition velocity is given by [WOO81], for which [AHM97] confirms a good match with experimental results.

$$v_{dep,turb} = u_\tau \cdot \left(0{,}057 \cdot Sc^{-\frac{2}{3}} + 4{,}5 \cdot 10^{-4} \cdot \tau^{+2}\right)$$

Here, u_τ is the friction velocity, Sc the Schmidt-number of the particles and τ^+ the dimensionless relaxiation time, which is derived from the particle relaxation time τ according to the following equation:

$$\tau^+ = \tau \cdot \frac{u_\tau^2 \cdot \rho_{fl}}{\eta}$$

In order to evaluate the importance of this mechanism, the pressure relief shaft was selected as a reference volume. Deposition as modeled with COCOSYS and integrated mass flow through the zone were taken from the calculation results; additionally, turbulent deposition was calculated with the correlation stated above and converted into deposited mass according to [HIN99].

The results are presented in table 4:

Table 4: Comparison of effects of implemented deposition models, turbulent deposition and integrated dust mass flow

	S1	S2	S3
Total dust mass deposited according to implemented models	$1.0 \cdot 10^{-5}\ g$	$1.1 \cdot 10^{-5}\ g$	$6.6 \cdot 10^{-6}\ g$
Total dust mass deposited due to turbulent deposition	$1.6 \cdot 10^{-3}\ g$	$1.6 \cdot 10^{-3}\ g$	$1{,}4 \cdot 10^{-3}\ g$
Integrated dust mass flow	$9.3\ g$	$11.0\ g$	$5.7\ g$

It can be seen that the dust mass on the surfaces due to turbulent deposition is two orders of magnitudes higher than due to all deposition models implemented in COCOSYS so far. Thus, a deposition mechanism with a high relevance for depressurization accidents of HTR is so far missing in this code system. However, it must be emphasized that the pressure relief shaft is a zone with high gas velocities which favor turbulent deposition , so the differences can be expected to be significantly lower in other zones. Also, a comparison of turbulent deposition with the integrated dust mass flow makes clear that the greatest part of the dust is still not deposited and remains gas borne. Thus, the results for released dust masses presented in chapter 4.1 are not expected to change much upon integration of turbulent deposition into COCOSYS. However, in order to generally qualify the code system for the simulation of HTR depressurization accidents, this addition would be worthwhile.

7.2.2 Resuspension

The only way to simulate resuspension in COCOSYS so far is via the Fromentin model based upon the work of [FRO89], [NOW08]. However, the goal of this implementation was to simulate the effect of pressure transients (e.g. from a hydrogen deflagration) on a pre-defined particle layer. [KLE10] Especially for a simulation of the interaction of deposition and resuspension, this approach is not suitable. An alternative would be the quasi-static Rock'n Roll model, which is also implemented in the STAR code as well as other severe accident codes like ASTEC [BUJ10].
For the case simulated here, modeling resuspension of dust deposited on confinement walls will not significantly increase the dust source term because deposition is already very low. For other accident scenarios, the effect might be more interesting, especially since the non-consideration of resuspension is intrinsically non-conservative. However, it must be emphasized that the challenge of identifying suitable particle adhesive force parameters faced for the STAR-simulation will also be faced for the containment code if resuspension is implemented.

7.2.3 Transfer of material values

So far, not all material values calculated in THY were actually available for the AFP calculation. For example, the molecular weight of the gas mixture and its thermal conductivity (actually, that value divided by the thermal conductivity of the particle) are to be entered by the user and remain constant during the whole simulation rather than using values from THY.

7.2.4 Characteristic lengths

In COCOSYS, the aerosol model uses a characteristic length of $3\ mm$ to calculate the temperature gradient for thermophoresis. It would be a significant improvement to replace that constant value with a simple calculation based upon the theory of heat transfer and applied e.g. by [STE10] and [JÜH11]:

By setting to equal the heat flux for the boundary layer and the heat transfer from fluid to wall, the following expression for the temperature gradient is obtained:

$$\dot{q}'' = \lambda_{fl} \cdot \nabla T$$
$$\dot{q}'' = \alpha \cdot (T_W - T_{fl})$$
$$\Leftrightarrow \nabla T = \frac{\alpha}{\lambda_{fl}} \cdot \left(T_W - T_{fl}\right)$$

The heat transfer coefficient α can be made available from the respective calculation in THY. However, an implementation into COCOSYS would require substantial validation efforts.

7.2.5 Input stucture of injection tables

The existing input structure of COCOSYS is clearly focused on injecting aerosol with a mathematically described (generally lognormal) particle size distribution. Creating injection tables for irregular, time-dependent size distributions is only possible with a disproportionate effort and by no means through simply including external files.
Simple improvements in the input routines could thus make the integration of aerosol injection data generated by primary circuit codes much easier, especially facilitating calculations with parameter variations.

7.2.6 Confinement model

Additionally to actual code improvements, the confinement model itself can still be optimized. Especially current experience with modeling plumes [BRO11] can be used to facilitate the simulation of actual gas flows with a minimum number of zones.

8 Summary and Perspective

The blow-down phase of a depressurization accident of an HTR has been simulated with COCOSYS. For the reference plant HTR-Module 200, the dust mass released into the environment has been calculated based upon a detailed modeling of the primary circuit not covered by this deliverable and the COCOSYS modeling of the confinement for a break of the pressure equalization line.
Based on the calculations performed, it can be stated that about two thirds of the dust released from the primary circuit are retained within the confinement; almost exclusively due to dust laden gas remaining in the building after pressure equalization while dust deposition is insignificant.

Turbulent deposition and dry resuspension have been identified as relevant mechanisms that are not covered yet by suitable COCOSYS models,. Their influence has been tentatively evaluated and found not to be decisive for the dust source term – however, their inclusion into COCSYS will contribute to reinforce its significance as a best-estimate code system. Together with some minor improvements concerning data handling, the potential for an optimization of the confinement model should be evaluated.

9 Literature

[AHM97] Ahmadi G., Chen Q.:*Deposition of particles in a turbulent pipe flow*, Journal of Aerosol Science, Vol. 28 Nr. 5, S. 789-796, 1997.

[AHM98] Ahmadi G., He C.: *Particle Deposition with Thermophoresis in Laminar an Turbulent Duct Flows*, Aerosol Science and Technology 29, S.525-546, 1998.

[ALL08] Allelein H.-J. et al.: *COCOSYS: Status of development and validation of the German containment code system*, Nuclear Engineering and Design 238, S. 872-889, 2008.

[BRO11] Broxtermann P., Allelein H.-J.: *Simulation of AP1000's Passive Containment Cooling with the German Containment Code System COCOSYS*, in: Proceedings of NENE2011, Bovec, Slovenia, 2011.

[BUJ10] Bujan A. etal.: *ASTEC V1.3 code SOPHAEROS module validation using the STORM experiments*, Progress in Nuclear Energy52, S. 777-788, 2010.

[CAR05] Carpick R.W., Grierson D.S., Flater E.E.: *Accounting for the JKR–DMT transition in adhesion and friction measurements with atomic force microscopy*, Journal of Adhesion Science and Technology, Vol. 19, Nr.3-5, S. 291-311, 2005.

[FAC08a] Fachinger J. et al.: *Examination of Dust in AVR Pipe Components*, Proceedings of the 4th International Topical Meeting on High Temperature Reactor Technology (HTR2008), Washington DC, USA, 28. September – 1.Oktober 2008.

[FAC08b] Fachinger J. et al. : Auswerteprotokolle zum Projekt „Dust Experiments on AVR Components“ (DEACO), 2008.

[FON09] Fontanet J. et al.: *Modelling of HTR Confinement Behavior during Accidents Involving Breach of the Helium Pressure Boundary*, Science and Technology of Nuclear Installations, Article ID 687634, Volume 2009, 2009.

[FRO89] Fromentin A. : *Particle Resuspension from a Multi-Layer Deposit by Turbulent Flow*, Programm LWR-Sicherheit, Paul Scherrer-Institut, PSI Bericht 38, Villingen 1989.

[GOR82] Goren S. L., D'Ottavio T.: *Aerosol Capture in Granular Beds in the Impaction Dominated Regime*, Aerosol Science and Technology 2, S. 91-108, 1982.

[GOT90] Gottaut H., Krüger K.: *Results of experiments at the AVR Reactor*, Nuclear Engineering and Design 121, S. 143-153, 1990.

[HER07] Herranz L. E., Del Prá C.L.: *Major challenges to modeling aerosol retention near a tube breach during steam generator tube rupture sequences*, Nuclear Technology,Vol. 158, S. 83-93, 2007.

[HIN99] Hinds C. W.: *Aerosol Technology – Properties, Behavior and Measurement of Airborne Particles*, John Wiley & Sons, Inc.,1999.

[IAE97] *Fuel performance and fission product behavior in gas cooled reactors*, IAEA-TECDOC-978, 1997.

[ING81] Ingham D.B.: *The diffusional deposition of aerosols in fibrous filters*, Journal of Aerosol Science, Vol. 12 Nr.4, S.357-365, 1981.

[INT560] *Aktivitätsfreisetzung und Strahlenexposition bei der HTR-Modul-Kraftwerksanlage – Teil I : Bestimmungsgemäßer Betrieb*, Technische Unterlagen für Gutachtergespräche, Ident-Nr. :76.00560.2, Interatom, 1987.

[INT561] *Aktivitätsfreisetzung und Strahlenexposition bei der HTR-Modul-Kraftwerksanlage – Teil II : Störfälle*, Technische Unterlagen für Gutachtergespräche, Ident-Nr. :76.00560.2, Interatom, 1988.

[INT679] *Belastungen des Reaktorgebäudes nach Rohrleitungsbrüchen*, Technische Unterlage entsprechend Unterlagenforderung, Ident-Nr. :76.00679.*, Interatom, 1988.

[INL11a] Pebble Bed Reactor Scoping Safety Study, Technical Data Record Document No.: 12 – 9149863 – 000, AREVA NP, available at: https://inlportal.inl.gov/portal/server.pt/document/78533/pebble_bed_reactor_scoping_safety_study_-_areva_pdf

[INL11b] Pebble Bed Reactor Plant Design Description, Technical Data Record Document No.: 12 – 9149697 – 000 , AREVA NP, available at: https://inlportal.inl.gov/portal/server.pt/document/78521/pebble_bed_reactor_plant_design_description_-_areva_pdf

[JÜH11] Jühe S.. : *Kohlenstoffstaubfreisetzung bei Druckentlastungsereignissen von Hochtemperaturreaktoren*, Dissertation, RWTH Aachen, 2011.

[JÜH12] Jühe S., Struth S., Schlögl B., Allelein H.-J.: Simulation of Dust Behavior in HTR with Pebble Bed Fuel, in: Proceedings TOPSAFE 2012.

[KLE10] Klein-Heßling W. et al.: *COCOSYS V2.4 User's Manual*, Gesellschaft für Anlagen- und Reaktorsicherheit, Köln, 2010.

[LÖF88] Löffler F.: *Staubabscheiden*, Thieme Verlag, Stuttgart, 1988.

[NOW08] Nowack H.: *Aerosolverhalten im Sicherheitsbehälter beim Einsatz von Rekombinatoren und nach Wasserstoffverbrennungen, Dissertation*, Bochum, 2008.

[OET89] Oetjen H.-F.: *Arbeitsprotokoll zu Behandlung der Proben und Bestimmung von Kornspektren an den THTR-Staubproben*, AP-6-89, Forschungszentrum Jülich, 1989.

[REE01] Reeks M. W., Hall D.: *Kinetic models for particle resuspension in turbulent flows: theory and measurement*, Journal of Aerosol Science 32, S. 1-31, 2001.

[SCE88] Scheibel H. G. et al.: *Untersuchungen der Spaltprodukt-Rückhaltung durch HTR-Reaktorschutzgebäude nach dem Vented-Confinement-Konzept*, Abschlussbericht BF-R-40.039-1.0, Battelle-Institut e.V. Frankfurt, 1988.

[STE10a] Stempniewicz M. M., Winters L., Caspersson S. A.: *Analysis of Dust and Fission Products in a Pebble Bed NGNP*, Proceedings of the 5th International Topical Meeting on High Temperature Reactor Technology (HTR2010), Prag, 18.-20. Oktober 2010.

[STE10b] Stempniewicz M. M.: *SPECTRA – Computer Code Manuals*, NRG, Arnhem, 2010.

[TAL80] Talbot L. et al.: *Thermophoresis of particles in a heated boundary layer*, Journal of Fluid Mechanics 101, S. 737-758, 1980.

[WOO81] Wood N.B.: *A simple Method for the calculation of turbulent deposition to smooth and rough surfaces*, Journal of Aerosol Science, Vol. 12 Nr. 3, S. 275-290, 1981.